Separation Science and Technology
Publication details, including instructions for authors and subscription information:
http://www.informaworld.com/smpp/title~content=t713708471

Effects of Poly(Vinyl Alcohol) Content and Calcination Temperature on the Characteristics of Unsupported Alumina Membrane

W. P. Yang[a]; S. S. Shyu[a]; En-Su Lee[a]; An-Chong Chao[b]
[a] DEPARTMENT OF CHEMICAL ENGINEERING, NATIONAL CENTRAL UNIVERSITY, CHUNG-LI, TAIWAN, REPUBLIC OF CHINA [b] DEPARTMENT OF CHEMICAL ENGINEERING, NATIONAL LIEN HO COLLEGE OF TECHNOLOGY AND COMMERCE, MIAO-LI, TAIWAN, REPUBLIC OF CHINA

To cite this Article Yang, W. P. , Shyu, S. S. , Lee, En-Su and Chao, An-Chong(1996) 'Effects of Poly(Vinyl Alcohol) Content and Calcination Temperature on the Characteristics of Unsupported Alumina Membrane', Separation Science and Technology, 31: 9, 1327 — 1343
To link to this Article: DOI: 10.1080/01496399608006954
URL: http://dx.doi.org/10.1080/01496399608006954

SEPARATION SCIENCE AND TECHNOLOGY, **31**(9), pp. 1327–1343, 1996

Effects of Poly(Vinyl Alcohol) Content and Calcination Temperature on the Characteristics of Unsupported Alumina Membrane

W. P. YANG, S. S. SHYU,* and EN-SU LEE
DEPARTMENT OF CHEMICAL ENGINEERING
NATIONAL CENTRAL UNIVERSITY
CHUNG-LI, TAIWAN 320, REPUBLIC OF CHINA

AN-CHONG CHAO
DEPARTMENT OF CHEMICAL ENGINEERING
NATIONAL LIEN HO COLLEGE OF TECHNOLOGY AND COMMERCE
MIAO-LI, TAIWAN, REPUBLIC OF CHINA

ABSTRACT

Nonsupported alumina porous membranes without pinholes or cracks were prepared by the sol–gel process using aluminum *sec*-butoxide as the starting material. The effects of using different PVA contents at various calcination temperatures on the characteristics of the membrane were investigated by scanning electron microscopy and nitrogen sorption porosimetry. The results after calcining at 450°C for 5 hours showed that the range of pore size distributions increases with increasing PVA concentration. The active nucleus numbers of phase transition to α-alumina decreased as the content of PVA increased at about 1050°C. The morphology of unsupported alumina membranes was affected by the PVA concentration and calcination temperature.

Key Words. Unsupported alumina membrane; Sol–gel process; Microstructure; Denucleation agent; Gas separation

* To whom correspondence should be addressed.

INTRODUCTION

During recent years the preparation of inorganic membranes has been the focus of much attention. Ceramic oxide membranes have been of special interest. Interesting advantages of such membranes over organic membranes are: thermal, chemical, and mechanical stability; resistance to microbial degradation; and a long life in service thanks to their ability to be cleaned by harsh media at high temperature (1–4). There are several processes for making ceramic membranes, e.g., chemical leaching, sol–gel, and solid-state calcining. The sol–gel technique is considered to be the most practical because their preparation leads to a low calcining temperature, a narrower pore size distribution, and a nanoscale pore diameter (5–8).

The sol-gel process has been applied to prepare porous membranes of alumina, silica, titania, zirconia, and silica-alumina (5, 9–19). Yoldas' reports (20–23) suggested the basic preparation condition of boehmite colloidal solution prepared from aluminum alkoxide via the sol–gel method and alumina monoliths prepared from this solution. After Yoldas, many investigators studied, in detail, all the stages of the sol–gel processing of alumina gels, the structure of gels, and their transformation to α-alumina (24–28). A number of later researchers attempted to influence the microstructure of alumina membrane by using various additives such as lanthanum, nickel, magnesium, silver, poly(vinyl alcohol) (PVA), resin, and acetic acid (5, 6, 18, 19, 29–31).

For this paper unsupported alumina porous membranes without defects were prepared by the modified sol–gel method, and several effects on the characteristics of these membranes were studied.

EXPERIMENTAL

Pure boehmite (r-AlOOH) sols were prepared using the procedure described by Yoldas (20–23). Aluminum tri-secondary butoxide (ATSB) was hydrolyzed by adding it to water in large excess (H_2O/alkoxide = 100 mol/mol) at 82°C while stirring vigorously. The solution was kept at 82°C, and 0.07 mol nitric acid per mol butoxide was added to peptize the sol colloids. After 1 hour the sol was kept boiling in an open reactor for a few hours to evaporate most of the butanol. It was subsequently refluxed overnight. Fresh deionized water was added to the sol to replace the evaporated water. The resulting sol was kept at room temperature before use.

Poly(vinyl alcohol) (PVA) (grade BF-24, $\overline{M}_n$ = 105,000) was obtained from Chang Chun Petrocochemical Co. and used as received. Solutions

with different PVA contents were prepared by adding various amounts of PVA (1, 3, 5 g, etc.) to 100 mL boiling water and stirring at high speed. After 4 hours refluxing, the PVA solution was mixed with pure boehmite sol (ratio: 1:4 v/v) to prepare a casting solution. A variety of dry films of the pre-membrane (PVA/[AlO(OH)]) were formed by casting the solution in a polystyrene Petri dish in filtered air at room temperature for about 9 to 14 days.

Seven films with thicknesses of about 180 μm were made by the above-mentioned procedure to give the following weight ratio of PVA/Al_2O_3: (a) 0, (b) 9.3, (c) 28.0, (d) 45, (e) 62.6, (f) 80, and (g) 115 wt%. These dry films were then calcined at a heating rate of 60°C/h with intermediate 2-hour plateaus at 200°C and a final one of 5 hours at different temperatures (230 to 1050°C).

The pore size distribution, pore volume (BJH method), average pore size, and surface area (BET method) for unsupported membrane samples were determined by nitrogen adsorption and desorption porosimetry (liquid-nitrogen temperature) (Micromeritics ASAP 2000). The morphology of some calcined membrane samples was analyzed by scanning electron microscopy (Hitachi S-2300).

RESULTS AND DISCUSSION

The microstructure of inorganic membranes with thicknesses of about 180 μm were studied by using different PVA amounts at various temperatures. Experimental observation after calcining shows that these films, except for pure boehmite, are able to form unsupported membranes of a crack-free layer. Their measurements of specific surface area, average pore size, and pore size distribution are shown in Table 1 and Figs. 1 to 7. Since unsupported membrane films with a PVA/Al_2O_3 ratio of 28 and 45 wt% which possess good mechanical strength can be used for further research on gas and pervaporation separation, they were studied in more detail than other membranes. The resulting morphology of unsupported membranes is presented in Figs. 8 and 9. The results are explained in the following sections.

The Influence of PVA Content in the Unsupported Membrane on the Microstructure

The adsorption and desorption isotherm curves for most unsupported membranes can be classified as type IV isotherms with a type E hysteresis loop (32). The type IV isotherm is the normal form of an isotherm and is found in porous substances with a pore diameter larger than 2 nm belong-

ing to the mesopore structure. Figure 1 presents typical N_2 adsorption–desorption isotherms for the PVA-added unsupported membrane after calcining at 450°C. The adsorption and desorption isotherm curves are linear when the relative pressure (P/P_0) is in the 0.05 to 0.35 range. The hysteresis effect loop appears when the relative pressure is more than about 0.35. The type E hysteresis loop is normally identified with ink-bottle-type pore. Uhlhorn's report (17) illustrates that this colloid suspension of pure boehmite consists of plate-shaped particles, and a card-packed dry film is obtained through precipitation. Therefore, the pores formed in the above dry film are very difficult to assign to a certain pore shape based on the type of hysteresis loop.

The adsorption gas volume of an unsupported alumina membrane increases with increasing PVA concentration, in general, at the same calcination temperature. After calcining at 450°C, the adsorption nitrogen gas volume of the non-added PVA membrane is about 140 cm^3/g (STP), and the adsorption gas volume evidently increases to about 280 cm^3/g (STP) when the PVA/Al_2O_3 ratio reaches 115 wt%, as shown in Fig. 1. The

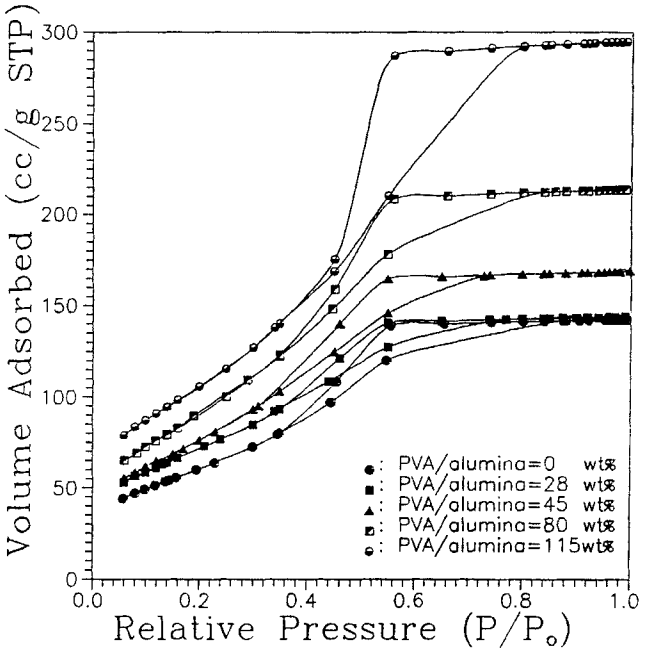

FIG. 1 Adsorption–desorption isotherms (N2) for unsupported membranes with different PVA/alumina ratios for calcining at 450°C.

hysteresis effect in the membrane increases with increasing adsorption volume. After calcining at 1050°C, the adsorption volume increases from 57 to 193 $cm^3/g(STP)$ as the ratio of PVA/Al_2O_3 increases from 0 to 115 wt%.

The pore size distribution can be calculated from the isotherm desorption by applying the Kelvin equation and using the BJH method. The various pore size distribution curves for the unsupported membrane after calcining at 450°C with different PVA additions are presented in Fig. 2. It shows that the pore size distribution peaks become sharper and more symmetrical with an increasing PVA/Al_2O_3 ratio. The pore diameters obtain from the Fig. 2 curves are less than 50 Å, which is independent of the PVA concentrations. Two reasons for this result should be considered: (a) PVA is a linear molecular with good main chain flexibility; (b) the pores formed from the boehmite, whose structure is card packed, are very strong, and therefore it is difficult to disrupt the pore structure. Thus, the added PVA should fill the formed pores. This leads to a sharper distribution of pore sizes, and so they have a similar pore diameter upper limit.

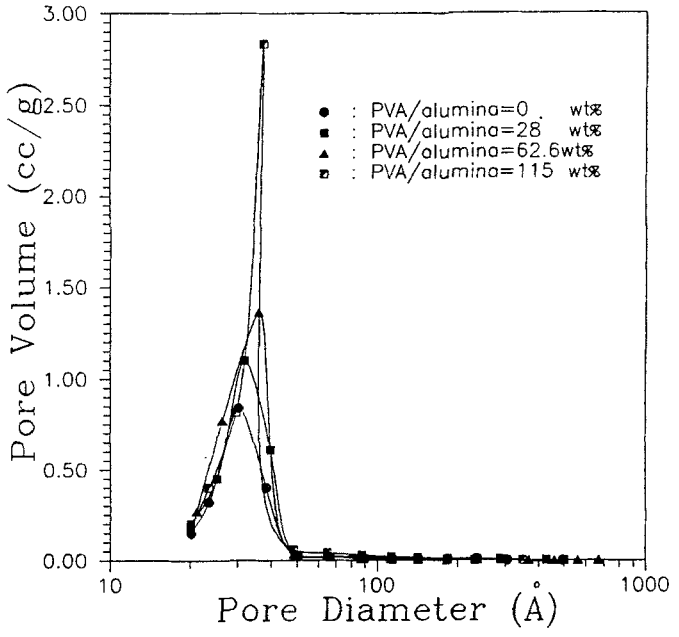

FIG. 2 Pore size distribution curves for unsupported membranes prepared with various PVA additions after calcining at 450°C.

The mean pore size and the narrow degree of pore size distribution can be controlled by using various peptizants as reported by Albani et al. (5). The preparation conditions for the above membrane is stricter than those for a membrane with PVA, especially the drying and calcining rate of the boehmite precursor films. Under such circumstances, the unsupported membrane formed without the addition of PVA are cracked.

The specific surface area (BET method) of the various membranes, as shown in Fig. 3, depends on the PVA/Al_2O_3 ratio. The maximum surface area occurs at about 350 and 450°C where the PVA content is increased slightly and greatly, respectively. Figure 4 illustrates the effects of different PVA amounts at various temperatures on the average pore diameter of the membranes. The data show that the structure changes a little when the PVA content increases slightly (≦28 wt%). The surface area increases with increasing temperature up to 350°C, and then reaches a maximum. But when the calcination temperature is higher than 350°C, the sintering phenomenon produces fused-deprecipitation and causes a significant increase in pore size and a decrease in surface area. Because the PVA/

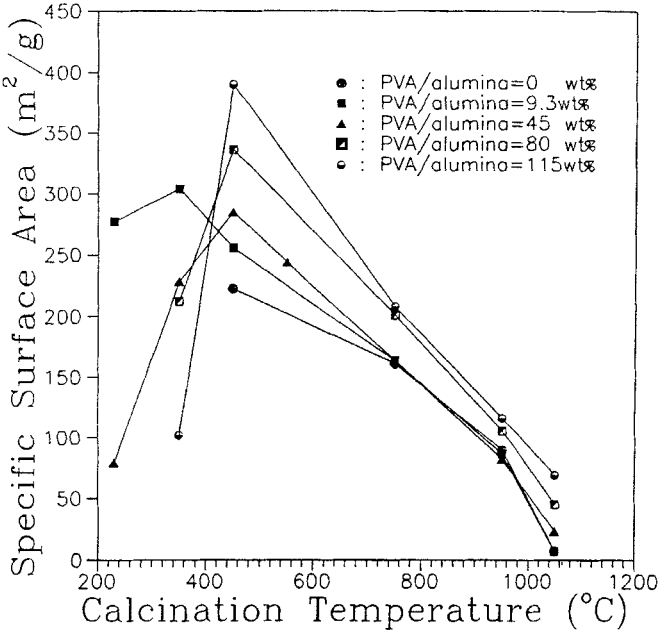

FIG. 3 The specific surface area as a function of the calcination temperature for several unsupported membranes.

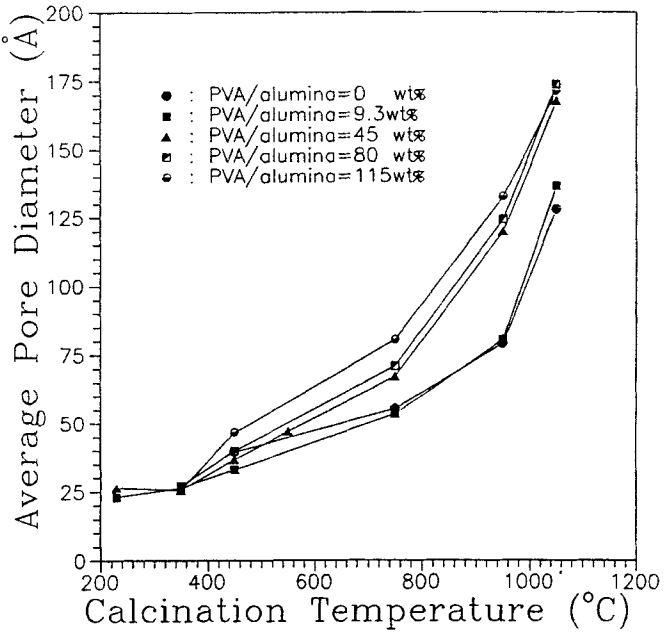

FIG. 4 The average pore diameter as a function of the calcination temperature for several unsupported membranes.

Al_2O_3 ratio is high (≧45 wt%), the structure changes greatly and the maximum surface area is located at 450°C.

Since PVA can be used as both a surfactant and a binder (33), it should reduce the internal space in the dried gel and decrease the surface tension of the gel during the drying and heating process. Therefore, a small amount of PVA can inhibited the increase in average pore size. Figure 4 and Table 1 show that these mean pore sizes (d) are 39.6 and 33 Å after calcining to 450°C for PVA/Al_2O_3 ratios of 0 and 9.3, respectively.

From Fig. 3 we also find that the various curves for different amounts of added PVA nearly converge at two different points after calcining at 750°C. It is suggested that the pore structure with a PVA/Al_2O_3 ratio of more than 45 wt% changes from one state to state after calcining at 750°C.

The Influence of Calcination Temperature in the Unsupported Membrane on the Microstructure

The adsorption and desorption isotherm curves for the membrane with PVA/Al_2O_3 = 45 wt% at different temperatures (230–950°C) are shown

TABLE 1
Mean Pore Size (d), Specific Surface Area (s), and Pore Volume (v) for Unsupported

Temperature (°C)	0 wt%			9.3 wt%			28 wt%		
	d (Å)	s (m^2/g)	v (cm^3/g)	d (Å)	s (m^2/g)	v (cm^3/g)	d (Å)	s (m^2/g)	v (cm^3/g)
230				23.1	277	0.128	21.8	144	0.048
350				26.4	304	0.198	26.8	311	0.197
450	39.6	222	0.235	33	255	0.232	33.5	266	0.245
550									
750	55.5	161	0.230	53.6	163	0.226	56.7	173	0.252
950	79.2	89.7	0.180	80.5	86.1	0.174	92	81.8	0.190

in Fig. 5. The curves of calcining at 230°C present a small hysteresis loop, and the hysteresis effect increases with the calcination temperature up to 750°C, reaches a maximum, and then decreases again at 950°C. According to the type of hysteresis loop, the pore shape of the membrane structure also changed from the ink-bottle type for calcining at 450°C to nearly the plate-shaped slit type with a narrower uniform distribution for calcining at 950°C.

The narrower pore size distribution of the membrane with PVA/Al_2O_3 = 45 wt% at various temperatures is shown in Fig. 6. In general, the mean pore size (except for pure boehmite) increases with the calcining temperature. According to Table 1, the average pore size changes in the 36.7 to 120 Å range as the temperature changes from 450 to 950°C. The slow pore growth and surface area decrease for these membranes at calcination temperatures lower than 950°C are caused by the normal sintering process (fused-deprecipitation phenomena), e.g., the formation of necks between crystallites by surface and volume diffusion. Therefore, the pore structure can be controlled by using different calcination temperatures.

It is interesting to note that the membrane sintered at 1050°C has a two-peak pore size distribution, which indicates the growth of a second group of pores in the macro-pore range. The membrane calcined at a temperature lower than 1050°C, however, did not show the two-peak pore size distribution (Fig. 6.) In order to understand this phenomenon, the various PVA-added membranes calcined at 1050°C for the same time are shown in Fig. 7. The substantial increase in pore size with a single-peak pore size distribution for the pure aluminum membrane calcined at 1050°C is believed to be the result of the complete phase transformation from r-Al_2O_3 (through δ-Al_2O_3 and θ-Al_2O_3) to α-Al_2O_3. Consequently, the single-peak

Membranes with Various Weight Ratios of PVA/Alumina at Different Temperatures

45 wt%			62.6 wt%			80 wt%			115 wt%		
d (Å)	s (m^2/g)	v (cm^3/g)	d (Å)	s (m^2/g)	v (cm^3/g)	d (Å)	s (m^2/g)	v (cm^3/g)	d (Å)	s (m^2/g)	v (cm^3/g)
26.4	79.4	0.047									
25.6	229	0.120	28.4	302	0.204	27.0	212	0.125	25.6	102	0.045
36.7	285	0.278	38.7	313	0.299	40.0	336	0.351	46.8	390	0.475
47.0	244	0.298									
67.4	164	0.281	74.3	187	0.351	71.1	201	0.363	80.7	208	0.426
120	81.9	0.246	133	94.9	0.302	124	106	0.325	133	116	0.379

pore size distribution is located in the macro-pore range. For the membrane with the PVA/Al_2O_3 = 115 wt%, however, the single-peak pore size distribution is located in the meso-pore range (d = 171.4 Å) and does not show the two-peak pore size distribution. Therefore, the phase

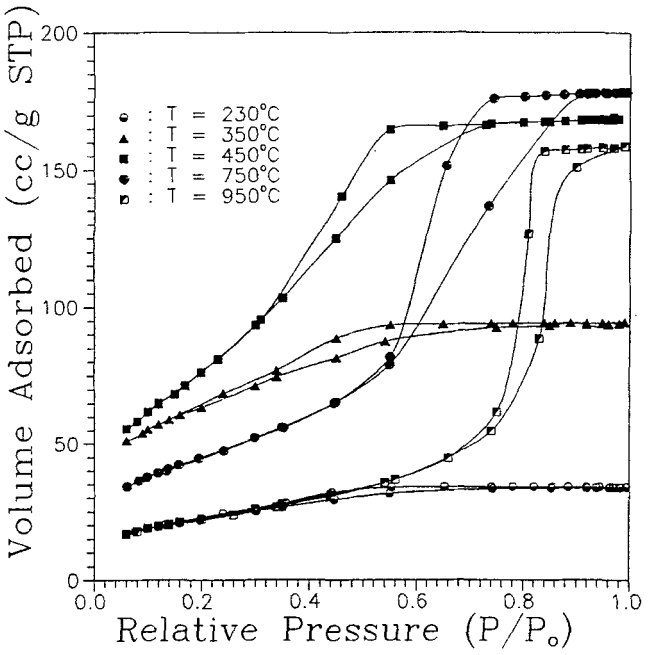

FIG. 5 Adsorption–desorption isotherms (N2) for calcining an unsupported membrane with PVA/alumina = 45 wt% at various temperatures.

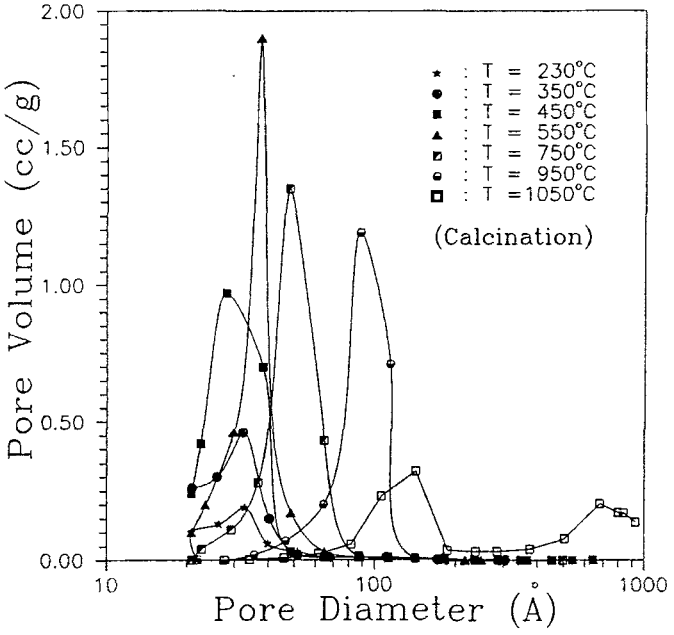

FIG. 6 Effects of calcining temperature on pore size distribution of an unsupported membrane with PVA/alumina = 45 wt%.

transformation from r-Al_2O_3 to α-Al_2O_3 did not occur and the existence of large PVA on the membrane may also raise the phase transformation temperature. The other types of membranes ($0 < PVA/Al_2O_3 < 115$ wt%) had a two-peak pore size distribution. The position of the secondary peak in the macro-pore range increased, and the intensity of this peak decreased as the PVA content increased. It is known that the phase transformation from γ-alumina to α-alumina proceeds via a nucleation and growth mechanism, with one nucleus being formed per crystallite. The active nucleus numbers of the phase transition to α-alumina could therefore decrease, causing the intensity of the secondary peak to decrease as the content of PVA increases after calcining at 1050°C. Theoretically, the PVA molecules of PVA-added films are burned out after calcining at less than 550°C. The efficiency of this transformation by nucleation is then controlled by the pre-membrane microstructures changing with the PVA content. As the content of PVA increases, the sintering behavior, which is accompanied by phase transformation, proceeds more easily, so the increase in the pore size of the secondary peak is more evident. According to Fig.

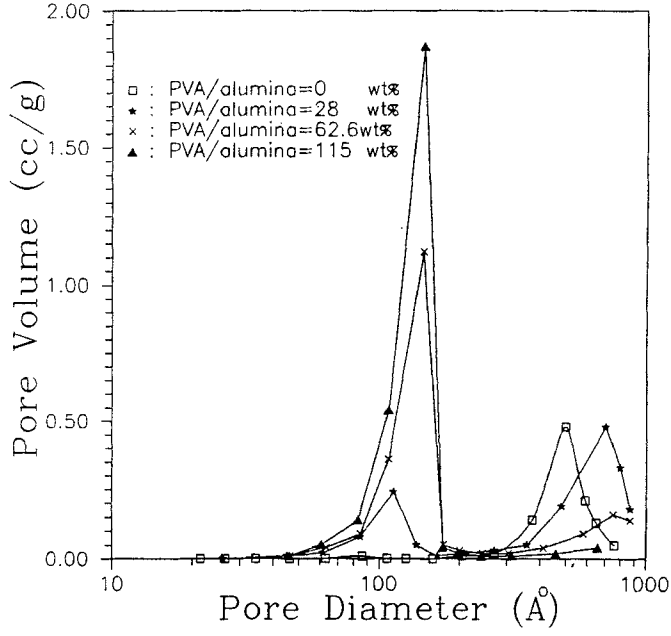

FIG. 7 Pore size distribution curves as a function of the PVA content for unsupported membrane calcining at 1050°C.

7, the positions of the secondary peak of the PVA/Al_2O_3 ratio of 0 and 45 wt% are located at about 500 and 850 Å, respectively. Pore sizes larger than 500 Å were measured by mercury porosimetry. In order to make the curves continuous and comparable with one another, we used the BJH method to detect the pore size although this method has larger errors when the pore size is bigger than 500 Å.

For a similar alumina membrane without PVA, mean pore diameters of about 46 and 22 Å were reported after sintering at 550°C for 2 hours and at 500°C for 24 hours, respectively (5, 9). The mean pore diameters were 31 and 30 Å for La-doped and undoped unsupported alumina membranes after calcining at 450°C for 3 hours, as reported by Lin (34). Larbot et al. (35) reported an increase in pore diameter from 50 to 100 Å for an unsupport alumina membrane (calcining time not given) as the sintering temperature was increased from 500 to 1000°C. Burggraaf and coworkers (17, 18) studied a PVA-added membrane with a fixed PVA content (PVA/Al_2O_3 = 25 wt%) at different calcination temperatures, and their explanation of the two points differs from ours.

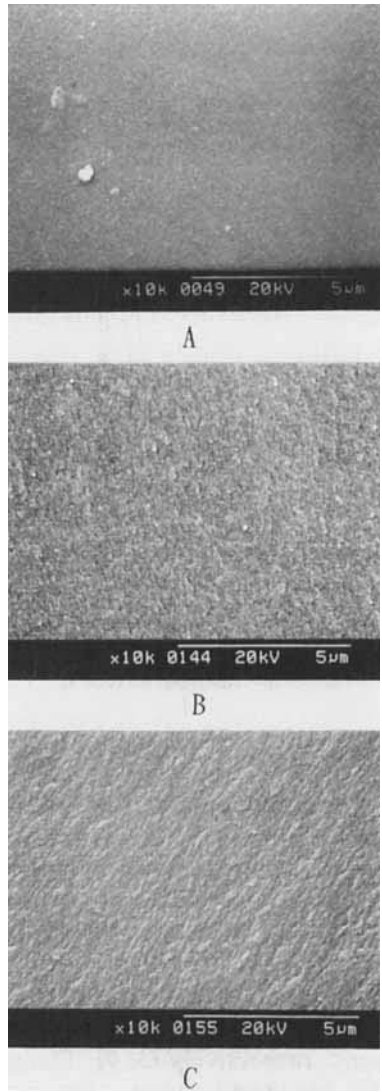

FIG. 8 SEM photographs of the surface (A) and fractured cross-section (B) of an unsupported membrane with PVA/alumina = 28 wt% after calcining at 450°C. SEM photograph C was obtained with PVA/alumina = 9.3 wt%.

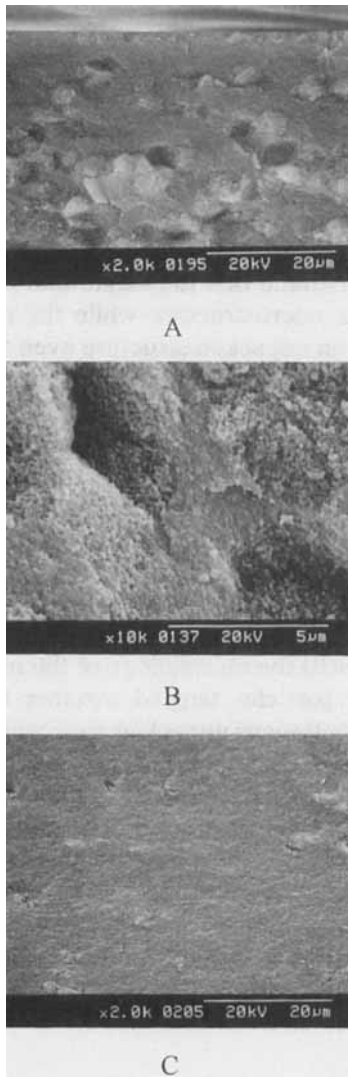

FIG. 9 SEM photographs of fractured unsupported membranes after calcining at 1050°C. A: Perpendicular view (× 2K) for PVA/alumina = 45 wt%. B: Amplified perpendicular view (× 10K) for PVA/alumnia = 45 wt%. C: Perpendicular view (× 2K) for PVA/alumina = 115 wt%.

Morphology Analysis

Morphological analysis were carried out using scanning election photomicrographs (SEM). Figures 8(A) and 8(B) show the SEM of an unsupported membrane with PVA/Al_2O_3 = 28 wt% after calcining at 450°C. In Fig. 8(A) the surface morphology shows no pinholes or craze. In Fig. 8(B) the fractured cross-section morphology has a uniform structure in general. These figures also indicate that both the aluminum colloid and PVA polymer chains are uniformly dispersed blends with no evident aggregation state. The SEM demonstrated that the membrane with PVA/$Al_2O_3 \leqq 9.3$ wt% has a more dense microstructure while the membrane with PVA/$Al_2O_3 \geqq 28.0$ wt% has an unpacked structure even though it was sintered at temperatures up to 950°C, as observed from a comparison of Figs. 8(B) and 8(C).

The SEM of the fractured cross-section of an unsupported membrane with PVA/Al_2O_3 = 45 wt% after calcining at 1050°C are shown in Figs. 9(A) and 9(B). These photographs indicates that large quadrate-like grains are dispersed uniformly in the internal structure. The membrane with PVA/Al_2O_3 = 115 wt% (Fig. 9C) does not have a large quadrate-like grains structure, but is like the structure at 950°C. The large quadrate-like grain, which is about 3.3 μm in length, is α-Al_2O_3 which has been transformed from γ-Al_2O_3. In Fig. 9(B) the morphology of the membrane shows long, small, cashew-nut-like particles tangled together to form quadrate-like grains, with a nearby continuous unpacked zone which is probably related to the presence of θ-Al_2O_3. The γ-phase transition to the δ- or θ-phase is reported by Wilson (36) for pure alumina calcined above 800°C.

Burggraaf and coworkers (18) showed that only a very small portion of the γ-alumina had become α-alumina in the small lanthanum-doped membrane at a sintering temperature of 1200°C, about 200°C higher than the transformation temperature of pure alumina gel, so there is a shift of about 200°C for the phase transition temperature. By comparing the lanthanum-doped and PVA-added membranes, it was found that the mechanisms for γ-Al_2O_3 transition to α-Al_2O_3 were different.

CONCLUSIONS

We demonstrated that the microstructure of a sol–gel derived unsupported alumina membrane could be controlled via interparticulate modification of boehmite sol at different calcination temperatures of the drying film. After calcining at 450°C, the sharp degree of pore size distribution increases with increasing PVA/Al_2O_3 ratio. The microstructure of the resulting unsupported membrane was easily influenced by PVA addition up

to PVA/Al_2O_3 = 45 wt%. For the various types of PVA-added membranes studied, the average pore size increased gradually with increasing calcining temperature when the calcining temperature was lower than 950°C. For the pure alumina membrane, the pore size increased substantially after calcining at 1050°C for 5 hours, which is attributed to phase transformation from γ-alumina to α-alumina. The phase transition to α-alumina could be decreased by increasing the PVA content under the same condition.

A morphologic study showed that the inner cross-section structure of such a membrane is systematic and uniform at calcining temperatures up to 950°C. Large quadrate-like α-alumina grains are dispersed uniformly in the internal structure of an alumina membrane calcined at 1050°C. Surface morphology showed no pinhole or craze in the PVA-added alumina membrane.

REFERENCES

1. H. K. Lonsdale, "The Growth of Membrane Technology," *J. Membr. Sci., 10*, 81 (1985).
2. R. R. Bhave, *Inorganic Membranes: Synthesis, Characteristics, and Applications*, Van Nostrand Reinhold, New York, 1991.
3. R. L. Goldsmith, "Guest Editorial," *J. Membr. Sci., 39*, 197–201 (1988).
4. A. S. Michaels, "Membrane, Membrane Processes, and Their Application: Needs, Unsolved Problems, and Challenges of the 1990's," *Desalination, 77*, 5–34 (1990).
5. M. I. D. Albani and C. P. Arciprete, "A Study of Pore Size Distribution and Mean Pore Size on Unsupported Gamma-Alumina Membrane Prepared by Modifications Introduced in the Alkoxide Hydrolysis Step," *J. Membr. Sci., 69*, 21–28 (1992).
6. T. Okubo, M. Watanabe, K. Kusakabe, and S. Morooka, "Nanostructural Control of Sol–Gel-Derived Porous Alumina via Modification of Sol," *J. Mater. Sci. Lett., 12*, 188–190 (1993).
7. C. J. Brinker, R. Sehgal, S. L. Hietala, R. Deshpande, D. M. Smith, D. Loy, and C. S. Ashley, "Sol–Gel Strategies for Controlled Porosity Inorganic Materials," *J. Membr. Sci., 94*, 85–102 (1994).
8. L. C. Klein and N. Giszpenc, "Sol–Gel Processing for Gas Separation Membranes," *Ceram. Bull., 169*(11), 1821–1825 (1990).
9. M. J. Gieselmann, M. A. Anderson, M. D. Moosemiller, and C. G. Hill Jr., "Physicochemical Properties of Supported and Unsupported γ-Al_2O_3 and TiO_2 Ceramic Membrane," *Sep. Sci. Technol., 23*, 1695–1714 (1988).
10. M. A. Anderson, M. J. Gieselmann, and Q. Xu, "Titania and Alumina Ceramic Membranes," *J. Membr. Sci., 39*, 243–258 (1988).
11. T. Okubo, M. Watanabe, K. Kusakabe, and S. Morooka, "Preparation of γ-Alumina Thin Membrane by Sol–Gel Processing and Its Characterization by Gas Permeation," *J. Mater. Sci., 25*, 4822–4827 (1990).
12. A. Julbe, C. Guizard, A. Larbot, L. Cot, and A. Giroir-Fendler, "The Sol–Gel Approach to Prepare Candidate Microporous Inorganic Membranes for Membrane Reactors," *J. Membr. Sci., 77*, 137–153 (1993).

13. M. P. Thomas, R. R. Landham, E. P. Butler, D. R. Cowieson, E. Barlow, and P. Kilmartin, "Inorganic Ultrafiltration Membranes Prepared by a Combination of Anodic Film and Sol–Gel Technologies," *Ibid.*, *61*, 215–225 (1991).
14. R. J. R. Uhlhorn, K. Keizer, and A. J. Burggraaf, "Gas Transport and Separation with Ceramic Membranes. Part II. Synthesis and Separation of Microporous Membranes," *Ibid.*, *66*, 271–287 (1992).
15. S. Kitao and M. Asaeda, "Separation of Organic Acid/Water Mixture by Thin Porous Silica Membrane," *J. Chem. Eng. Jpn.*, *23*, 367–370 (1990).
16. C. J. Brinker, T. L. Ward, R. Sehgal, N. K. Raman, S. L. Hietala, D. M. Smith, D. W. Hua, and T. J. Headley, "Ultramicroporous Silica-Based Supported Inorganic Membranes," *J. Membr. Sci.*, *77*, 165–179 (1993).
17. R. J. R. Uhlhorn, M. H. B. J. Huis Int Veld, K. Keizer, and A. J. Burggraaf, "Synthesis of Ceramic Membranes. Part I Synthesis of Nonsupported and Supported γ-Alumina Membranes without Defects," *J. Mater. Sci.*, *27*, 527–537 (1992).
18. Y. S. Lin, K. J. de Vries, and A. J. Burggraaf, "Thermal Stability and Its Improvement of the Alumina Membrane Top-Layers Prepared by Sol–Gel Methods," *Ibid.*, *26*, 715–720 (1991).
19. J. Etienne, A. Larbot, A. Julbe, C. Guizard, and L. Cot, "A Microporous Zirconia Membrane Prepared by the Sol–Gel Process from Zirconyloxalate," *Ibid.*, *86*, 95–102 (1994).
20. B. E. Yoldas, "A Transparent Porous Alumina," *Cerami. Bull.*, *54*, 286–288 (1975).
21. B. E. Yoldas, "Alumina Sol Preparation from Alkoxides," *Ibid.*, *54*, 289–290 (1975).
22. B. E. Yoldas, "Alumina Gels That Form Porous Transparent Al_2O_3," *J. Mater. Sci.*, *10*, 1856–1860 (1975).
23. B. E. Yoldas, "Hydrolysis of Alumina Alkoxides and Bayerite Conversion," *J. Appl. Chem. Biotechnol.*, *23*, 803–809 (1973).
24. Z. Jaworska-Galas, S. Janiak, W. Mista, J. Wrzyszcz, and M. Zawadzki, "Morphological and Phase Changes of Transition Alumina during Their Rehydration," *J. Mater. Sci.*, *28*, 2075–2078 (1993).
25. L. Radonjic, V. Srdic, and L. Nikolic, "Relationship between the Microstructure of Boehmite Gels and Their Transformation to α-Alumina," *Mater. Chem. Phys.*, *33*, 298–306 (1993).
26. M. Iwasaki, M. A. Yasumori, H. Kawazoe, and M. Yamane, "Thermal Properties of Gel-Derived Materials of Al_2O_3–SiO_2 System," *J. Non-Cryst. Solids*, *121*, 147–152 (1990).
27. A. C. Pierre and D. R. Uhlmann, "Amorphous Aluminum Hydroxide Gels," *Ibid.*, *82*, 271–276 (1986).
28. B. S. Maruthiprasad, M. N. Sastri, S. Rajagopal, K. Seshan, K. R. Krishnamurthy, and T. S. R. Prasada Rao, "Thermal Analysis of Alumina Precursors Prepared by 'PFHS' Methods," *J. Therm. Anal.*, *34*, 1023–1030 (1988).
29. R. J. R. Uhlhorn, V. T. Zaspalis, K. Keizer, and A. J. Burggraaf, "Synthesis of Ceramic Membranes. Part II. Modification of Alumina Thin Films: Reservoir Method," *J. Mater. Sci.*, *27*, 538–552 (1992).
30. Z. D. Ziaka, R. G. Minet, and T. T. Tsotsis, "A High Temperature Catalytic Membrane Reactor for Propane Dehydrogenation," *J. Membr. Sci.*, *77*, 221–232 (1993).
31. J. Zaman and A. Chakma, "Inorganic Membrane Reactors," *Ibid.*, *92*, 1–28 (1994).
32. K. S. W. Sing, D. H. Everett, R. A. W. Haul, L. Moscou, R. A. Pierotti, J. Rouquerol, and T. Siemieniewska, "Reporting Physisorption Data for Gas/Solid Systems with Special Reference to the Determination of Surface Area and Porosity," *Pure Appl. Chem.*, *57*, 603 (1985).

33. J. S. Reed, *Introduction to the Principles of Ceramic Processing*, Wiley, New York, 1989, pp. 152–166.
34. Y. Lin, C. Chang, and R. K. Gopalan, "Improvement of Thermal Stability of Porous Nanostructureed Ceramic Membranes," *Ind. Eng. Chem. Res.*, *33*, 860–870 (1994).
35. A. Larbot, J. P. Fabre, C. Guizard, and L. Cot, "Inorganic Membranes Obtained by Sol–Gel Techniques," *J. Membr. Sci.*, *39*, 203 (1988).
36. S. J. Wilson, "Phase Transformations and Development of Microstructure in Boehmite-Derived Transition Aluminas," *Br. Ceram. Soc. Proc.*, *28*, 281 (1979).

Received by editor August 16, 1995